Laser cooling of optically trapped molecules

Loïc Anderegg[1,2]*, Benjamin L. Augenbraun[1,2], Yicheng Bao[1,2], Sean Burchesky[1,2], Lawrence W. Cheuk ⬤[1,2], Wolfgang Ketterle[2,3] and John M. Doyle[1,2]

Ultracold molecules are ideal platforms for many important applications, ranging from quantum simulation[1-5] and quantum information processing [6,7] to precision tests of fundamental physics[2,8-11]. Producing trapped, dense samples of ultracold molecules is a challenging task. One promising approach is direct laser cooling, which can be applied to several classes of molecules not easily assembled from ultracold atoms[12,13]. Here, we report the production of trapped samples of laser-cooled CaF molecules with densities of 8×10^7 cm^{-3} and at phase-space densities of 2×10^{-9}, 35 times higher than for sub-Doppler-cooled samples in free space[14]. These advances are made possible by efficient laser cooling of optically trapped molecules to well below the Doppler limit, a key step towards many future applications. These range from ultracold chemistry to quantum simulation, where conservative trapping of cold and dense samples is desirable. In addition, the ability to cool optically trapped molecules opens up new paths towards quantum degeneracy.

Heteronuclear bialkali molecules assembled from ultracold atoms have been brought near quantum degeneracy in recent years and have enabled the study of long-range dipolar interactions and quantum-state-controlled chemistry[15,16]. It is desirable to control other kinds of molecule as they can offer new desirable features. One such class of molecules are those with unpaired electron spins (for example, those with $^2\Sigma$ ground states), which lead to both a non-zero electric and magnetic moment. Such molecules are important for quantum simulation, as they can be used to simulate a large variety of lattice spin models[3], and for quantum information[4]. Recently, laser cooling and magneto-optical trapping of two $X^2\Sigma$ molecules, CaF and SrF (refs [17–21]), were reported. For a wide variety of applications ranging from precision spectroscopy to quantum information, trapping in a conservative trap is needed.

Conservative traps in ultracold atom experiments are commonly formed from magnetic or optical fields. Recently, magnetic trapping of laser-cooled molecules was reported[14,22]. The significant advantages of magnetic traps are large volumes and high trap depths, which open up the possibility of further evaporative or sympathetic cooling. Optical traps, despite their much smaller trap volumes and lower trap depths, can be used to trap molecules regardless of their internal state. This allows for the possibility of further laser cooling of trapped samples, which, as demonstrated in this work, can lead to significant enhancement in density and phase-space density. It also opens up new methods towards quantum degeneracy, some of which can occur on much shorter timescales and be more efficient than evaporative cooling. For example, laser cooling of optically trapped atoms has recently led to the production of Bose–Einstein condensates without evaporation[23,24]. Nevertheless, in most cases, the cooling in the optical trap is impeded by the different a.c. Stark shifts for ground and excited states. Here, we show that CaF (and

similar molecules) have a favourable level structure that allows for efficient cooling while optically trapped. Another key advantage of optical traps is their flexibility. Arbitrary small-scale features on the order of the wavelength of the trapping light can be created.

The starting point of our experiment is a radio-frequency magneto-optical trap (MOT) of CaF molecules loaded from a cryogenic buffer gas beam. This set-up has been described previously[21], except that here we implement chirped slowing of the CaF molecular beam[25]. The radio-frequency MOT is the same, operating on the $X^2\Sigma^+$ ($N=1$)$\rightarrow$$A^2\Pi_{1/2}$($J'=1/2$) transition, and consists of three retro-reflected MOT beams, along with lasers to repump out of the $v=1$, 2, 3 vibrational levels. In addition to forming the radio-frequency MOT, the MOT beams are also used for sub-Doppler cooling. Each MOT beam has a $1/e^2$ diameter of 9 mm and contains 30 mW of $X(v=0)\rightarrow A(v=0)$ light and 30 mW of $X(v=1)\rightarrow A(v=0)$ light. The power distribution among hyperfine components, addressed with acousto-optic modulators (AOMs), for both $X(v=0, 1)\rightarrow A(v=0)$ are 18%, 36%, 36% and 10% for the states $|J, F\rangle = |3/2, 1\rangle$, $|3/2, 2\rangle$, $|1/2, 1\rangle$ and $|1/2, 0\rangle$, respectively. When loading molecules into the radio-frequency MOT, the MOT beams are detuned from resonance by $\Delta_{MOT}=-2\pi \times 9$ MHz (Fig. 1b). The MOT beams are initially held at full intensity for 15 ms, capturing 10^5 molecules into the MOT. The intensity of each MOT beam is then reduced by a factor of 8 over 30 ms. Lower intensities reduce the sub-Doppler heating associated with red detuning on a $J\rightarrow J$ or $J\rightarrow J-1$ transition[26] and decrease the MOT temperature from 2 mK to 0.35 mK while increasing the density to 5×10^6 cm^{-3}.

The inverted angular momentum structure of CaF is similar to the D_1 line in alkali atoms, and allows for further cooling at blue detunings[20,26–28]. To perform sub-Doppler cooling, the MOT beams and the MOT magnetic gradient are switched off in 200 µs, during which time the laser is detuned to the blue, $\Delta_{SD} \approx +3\Gamma$ ($\Gamma = 2\pi \times 8.3$ MHz). The MOT beams, with polarization switching turned off, are then switched back on at full intensity, but without the $J=3/2,F=1$ component (Fig. 1b), which can lead to heating as it is red-detuned relative to the $J=1/2,F=0$ transition. Repumping out of $|3/2,1\rangle$ is still accomplished, albeit at a reduced rate by off-resonant light that nominally addresses the $|3/2,2\rangle$ state. For optimal cooling, compensation coils are used to cancel ambient magnetic fields to better than 0.1 G. In a time of ~100 µs, the molecules are cooled to 40 µK, much lower than the Doppler cooling limit of 200 µK.

After sub-Doppler cooling, we load the molecules into a far-detuned optical dipole trap (ODT). The ODT is formed from 12.7 W of single-frequency 1,064 nm light focused to a Gaussian beam waist of 29 µm, which produces a trap with a calculated depth of 380(60) µK, with radial (axial) trap frequencies of $2\pi \times 2.5$ kHz ($2\pi \times 21$ Hz). The ODT light is reflected by a dichroic mirror that transmits the fluorescence of the molecules, which is imaged onto
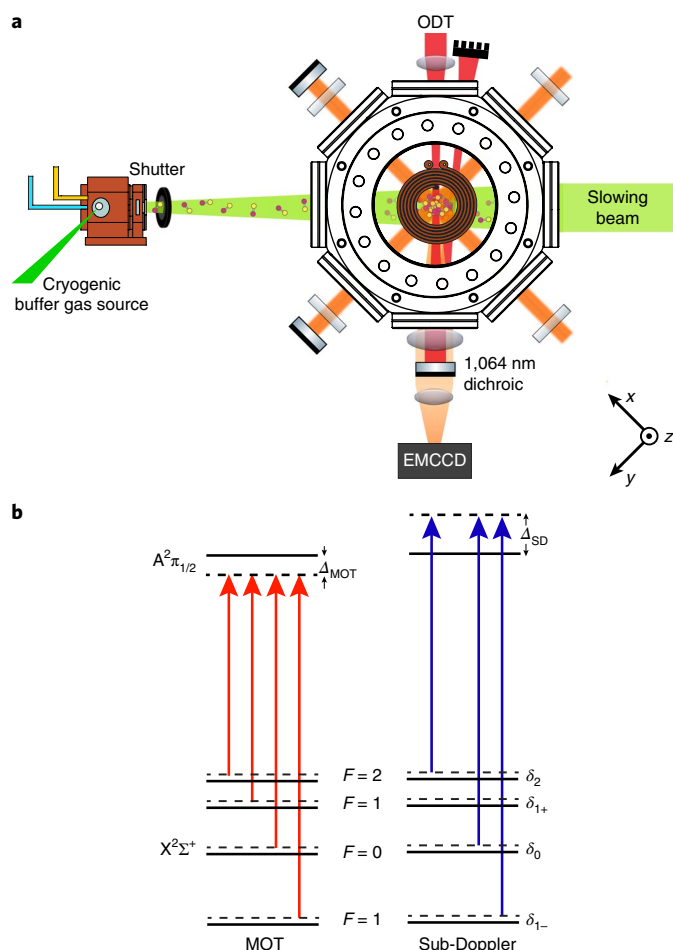
Fig. 1 | Schematic of experimental apparatus and level diagram for sub-Doppler cooling of CaF. a, Layout of the experimental apparatus. See ref. [21] for details. **b**, Laser detunings for the radio-frequency MOT and for sub-Doppler cooling. For the radio-frequency MOT, the light is detuned by $\Delta_{MOT} = -2\pi \times 9$ MHz; for sub-Doppler cooling, the light is detuned by $\Delta_{SD} = 2\pi \times 28$ MHz. The individual hyperfine sidebands are addressed with AOMs, and have detunings of $\{\delta_2, \delta_{1^+}, \delta_0, \delta_{1^-}\} = 2\pi \times \{1.8, 0, 0, -4.3\}$ MHz. Positive detunings correspond to blue detunings relative to the respective resonances for the various hyperfine components.
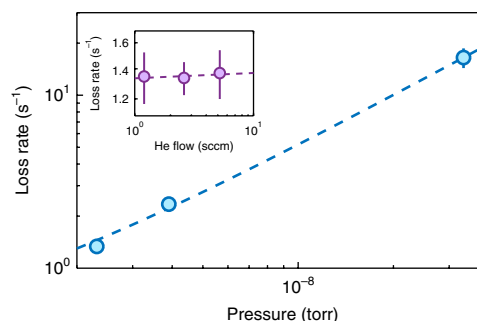

Fig. 2 | Loss rate of molecules trapped in the ODT. The inset shows the loss rate as a function of the buffer gas flow rate. We observe negligible effect of increasing the buffer gas flow, but significant dependence on the background pressure. The dependence of loss rate on buffer gas flow is measured to be 0.0(2) s^{-1} sccm^{-1}, while the dependence on background pressure is 5.5(1) $\times 10^8$ s^{-1} Torr^{-1}. The error bars represent the standard error of the fitted value. Dashed lines show linear fits.

an electron-multiplying charge-coupled device (EMCCD) camera (Fig. 1a). The reflected ODT beam is directed to a beam dump, away from the trapped molecules.

To capture molecules in the optical trap, the ODT light is switched on at the start of the sub-Doppler cooling. The sub-Doppler light is then ramped down in intensity by 30% in the first 10 ms and left on for a further 5 ms. We wait for 50 ms to allow untrapped molecules to fall from the imaging region, before imaging using a 0.5 ms pulse of light resonant with the X→A transition. With optimal parameters, 150(30) molecules are transferred into the ODT. The number of transferred molecules is determined by the size of the optical trap (29 μm waist), which is much smaller than the size of the initial sub-Doppler-cooled cloud (~2 mm full-width at half-maximum (FWHM)). For a given trap depth, the size of the trap is limited by the total available laser power, a technical limitation that can be overcome in future experiments. For the trapped molecules, we measure a temperature of 60 μK. Using the measured ODT beam profile and the number of trapped particles, we determine the peak density in the trap to be 8(2) $\times 10^7$ cm^{-3}, one order of magnitude higher than in the MOT. Our estimation is obtained by assuming

thermally distributed molecules in the trapping potential of the ODT, and agrees with classical Monte Carlo simulations of particles drawn from a uniform density distribution at the experimentally measured sub-Doppler temperature. This corresponds to a peak phase-space density of 2 $\times 10^{-9}$, three times higher than in the free-space sub-Doppler-cooled cloud.

An important characteristic of the ODT is the lifetime of trapped molecules, which is measured to be 750(40) ms (1/e decay time), shorter than the calculated lifetime ($\gg$ 1 s) due to heating from off-resonant photon scattering of the 1,064 nm ODT light. To determine what limits the lifetime, we vary the flow rate of helium into the buffer gas cell, with no appreciable effect on the lifetime (Fig. 2 inset). An in-vacuum shutter that is open for <10 ms during each experimental cycle eliminates the effects of buffer gas collisions on the 1 s timescale. To explore the dependence of loss rate on background pressure, we vary the MOT chamber pressure from 1×10^{-9} Torr to 3×10^{-8} Torr and find a dependence of 5.5(1) $\times 10^8$ s^{-1} Torr^{-1} (Fig. 2). This indicates that at our current operating conditions of 1×10^{-9} Torr, the loss rate of molecules from the ODT is dominated by collisions with background gas.

We further characterize the effect of the sub-Doppler light on the ODT loading process. We first vary the frequency of the sub-Doppler cooling light during ODT loading. As shown in Fig. 3, optimal loading occurs when the sub-Doppler cooling light is detuned +3 MHz relative to the free-space cooling frequency that produces the lowest temperature. The detuning is consistent with estimates of the a.c. Stark shift on the X→A transition arising from the ODT.

We next vary the overlap duration of the cooling light and the ODT. This is accomplished as follows. We shorten the sub-Doppler intensity ramp to 2 ms with the ODT off. Subsequently, the ODT is switched on, and we vary the amount of time that the sub-Doppler light overlaps with the ODT light. Zero temporal overlap corresponds to direct capture of sub-Doppler-cooled molecules. As shown in Fig. 4, we find that the number of trapped molecules increases by up to a factor of 5 and reaches a peak at 5 ms. To verify that the enhancement is not due to additional sub-Doppler cooling in free space, we increase the duration of the free-space sub-Doppler cooling by an additional 5 ms before switching on the ODT. With the additional free-space cooling, we find a smaller initial number of loaded molecules, likely due to a lower central density resulting from the longer sub-Doppler-cooling time. Despite a smaller initial number, the number of loaded molecules again rises as a function of overlap time. The peak number is reached at ~10 ms, at a similar level to the case without extra sub-Doppler cooling.
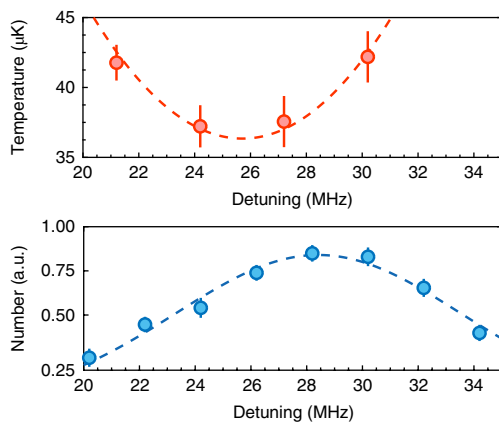
Fig. 3 | Dependence of sub-Doppler cooling and ODT loading on laser detuning. Top: free-space sub-Doppler temperature as a function of detuning Δ_{SD}. The dashed line shows a quadratic fit. Bottom: number of trapped molecules in the ODT as a function of Δ_{SD}. The dashed line shows a Gaussian fit. We observe a 3 MHz shift between optimal ODT loading and optimal free-space sub-Doppler cooling, which is consistent with the estimated a.c. Stark shift due to the ODT. The error bars represent the standard error of the fitted value.
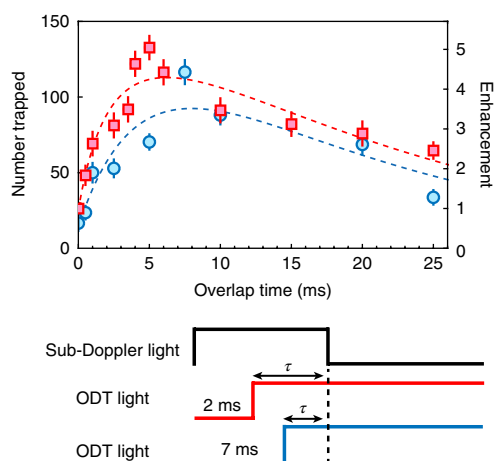

Fig. 4 | Loading of molecules into the ODT as a function of overlap time, τ, with the sub-Doppler light. Shown in red squares (blue circles) is the number loaded when the cooling light is turned on 2 ms (7 ms) before the ODT light. The error bars represent the standard error of the fitted value. The number of molecules loaded into the ODT is enhanced by up to a factor of 5 with sub-Doppler light. The enhancement is relative to $\tau = 0$ for 2 ms of free-space cooling. The dashed lines indicate fits to a rate equation model, with constant loss rate and loading rate proportional to τ. The bottom schematic shows the relative timing of the sub-Doppler light and the ODT light.

The initial rise at short times indicates that there is a time window of ~10 ms when molecules that pass by the ODT can be cooled by sub-Doppler light into the trap. The optimal loading time coincides with the average time it takes for a molecule on one edge of the initial sample to traverse the optical trap, where it can be cooled into the trap. Since the ODT is a conservative trap, the enhanced loading suggests that cooling is occurring at least in some region of the trap. Another indication of sub-Doppler cooling of trapped molecules is that the measured temperature of 60(5) μK is significantly lower than that expected from direct capture (100 μK).
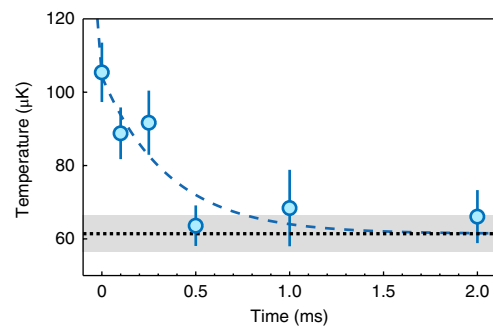

Fig. 5 | Cooling of optically trapped molecules. Trapped molecules are heated by a 40 μs pulse of resonant light at time $t = 0$. Shown in blue circles is the temperature as a function of varying sub-Doppler cooling time beginning at $t = 0.2$ μs. An exponential fit, shown by the dashed blue line, yields a 1/e time constant of ~300 μs. The temperature before heating is indicated by the black dotted line, with the standard error indicated by the shaded region. The error bars represent the standard error of the fitted temperature.

To directly demonstrate that cooling is occurring in the presence of the trap light, we heat the CaF molecules to ~100 μK by applying a 40 μs pulse of resonant light (detuned by +3 MHz to compensate for the Stark shift of the ODT beam). To ensure that the heated molecules are trapped, we measure the molecule number after waiting 50 ms. After the resonant heating pulse is applied, half of the trapped molecules remain. We then apply a pulse of sub-Doppler-cooling light and observe that the molecules are re-cooled to ~60 μK with a 1/e time of ~300 μs (Fig. 5). This verifies that sub-Doppler cooling works for molecules trapped in the ODT. This is an important initial demonstration, as successful laser cooling of trapped molecules can pave the way towards highly efficient means to create dense ultracold samples. At the currently achieved densities, laser cooling is nearly lossless and, unlike evaporative cooling, is independent of collisional properties. Since entropy in the system is continuously and quickly removed, higher phase-space densities can be reached with minimal loss. For example, by compressing the sample in the presence of cooling, the density could be increased with no rise in temperature.

We have observed that the temperature reached by sub-Doppler cooling of optically trapped molecules is higher than that attained in free space, as has also been observed in alkali atoms. Although sub-Doppler cooling via gray molasses is well understood in free space[26,27], in an optical trap, a.c. Stark shifts can interfere with cooling. We show here that sub-Doppler cooling in an ODT is possible, albeit reaching a temperature slightly higher than that attained in free space. The difference can arise from the spatial inhomogeneity of the Stark shifts, which prevents the entire sample from being at the optimal detuning. A further complication is that the Stark shifts are slightly state-dependent, which impede cooling by dephasing the dark states present in gray-molasses cooling. While state-dependent Stark shifts can be avoided for ground-state alkali atoms by using linearly polarized trapping light, they are unavoidable for molecular states with non-zero tensor Stark shifts.

In the future, lower sub-Doppler temperatures will allow for better transfer to, and cooling in, the ODT. This can be achieved with lambda-enhanced gray molasses, which has been demonstrated in atoms to provide temperatures a few times the recoil limit[28–30]. For CaF molecules, this temperature corresponds to ~5 μK, an order of magnitude lower than reported here. Lower temperatures reduce the required trap depth, which results in smaller state-dependent Stark shifts and allows for larger trap volumes to be used.

In conclusion, we have demonstrated loading of laser-cooled CaF (X²Σ) molecules into an optical dipole trap and the sub-Doppler

laser cooling of optically trapped molecules in the microkelvin regime. The approach in this work is applicable to a large class of molecules, including polyatomic species, for example SrOH, YbOH, $CaOCH_3$, $CaOCH(CH_3)_2$ (refs [11,13,31]). One immediately accessible application is the study of collisions and reactions of ground-state molecules with atoms[32]. One could explore the possibility of spin control of chemical reactions, for example between CaF and Li (ref. [33]), or proposed techniques such as collisional 'shielding'[34]. The study of molecule–molecule collisions is also within reach. With future improvements, one could produce samples sufficiently dense (10^9 cm^{-3}) for loading an optical tweezer with a typical trap volume of $10\,\mu m^3$ (refs [35,36]). Laser cooling and photon cycling of trapped molecules will be important for such experiments, as it enables optical readout of single molecules, where many photons must be scattered with minimal heating. Extensions to arrays of optical tweezers of molecules would provide a pristine environment in which quantum simulation and quantum computation can be performed[5,37,38]. New avenues to quantum degeneracy are also made possible with optically trapped molecules. In tightly confining potentials, it becomes possible to perform Raman sideband cooling or electromagnetically induced transparency (EIT) cooling, both highly efficient cooling methods that can circumvent the need for large initial numbers in traditional evaporative cooling schemes[39–42]. Our work is thus a significant step towards applications ranging from quantum simulation to ultracold chemistry.

Data availability

The data that support the plots within this paper and other findings of this study are available from the corresponding author upon reasonable request.

References

1. Micheli, A., Brennen, G. K. & Zoller, P. A toolbox for lattice-spin models with polar molecules. *Nat. Phys.* **2**, 341–347 (2006).
2. Carr, L. D., DeMille, D., Krems, R. V. & Ye, J. Cold and ultracold molecules: science, technology and applications. *New J. Phys.* **11**, 055049 (2009).
3. Pupillo, G. et al. Cold atoms and molecules in self-assembled dipolar lattices. *Phys. Rev. Lett.* **100**, 050402 (2008).
4. Büchler, H. P. et al. Strongly correlated 2D quantum phases with cold polar molecules: controlling the shape of the interaction potential. *Phys. Rev. Lett.* **98**, 060404 (2007).
5. Blackmore, J. A. et al. Ultracold molecules: a platform for quantum simulation. Preprint at http://arXiv.org/abs/1804.02372v1 (2018).
6. DeMille, D. Quantum computation with trapped polar molecules. *Phys. Rev. Lett.* **88**, 067901 (2002).
7. Yelin, S. F., Kirby, K. & Côté, R. Schemes for robust quantum computation with polar molecules. *Phys. Rev. A* **74**, 050301 (2006).
8. ACME Collaboration Order of magnitude smaller limit on the electric dipole moment of the electron. *Science* **343**, 269–272 (2014).
9. Kara, D. M. et al. Measurement of the electrons electric dipole moment using YbF molecules: methods and data analysis. *New J. Phys.* **14**, 103051 (2012).
10. Lim, J. et al. Laser cooled YbF molecules for measuring the electron's electric dipole moment. *Phys. Rev. Lett.* **120**, 123201 (2018).
11. Kozyryev, I. & Hutzler, N. R. Precision measurement of time-reversal symmetry violation with laser-cooled polyatomic molecules. *Phys. Rev. Lett.* **119**, 133002 (2017).
12. Rosa, M. D. Laser-cooling molecules. *Eur. Phys. J. D* **31**, 395–402 (2004).
13. Kozyryev, I., Baum, L., Matsuda, K. & Doyle, J. M. Proposal for laser cooling of complex polyatomic molecules. *ChemPhysChem* **17**, 3641–3648 (2016).
14. Williams, H. J. et al. Magnetic trapping and coherent control of laser-cooled molecules. *Phys. Rev. Lett.* **120**, 163201 (2018).
15. Yan, B. et al. Observation of dipolar spin-exchange interactions with lattice-confined polar molecules. *Nature* **501**, 521–525 (2013).
16. Ospelkaus, S. et al. Quantum-state controlled chemical reactions of ultracold potassium-rubidium molecules. *Science* **327**, 853–857 (2010).
17. Barry, J. F., McCarron, D. J., Norrgard, E. B., Steinecker, M. H. & DeMille, D. Magneto-optical trapping of a diatomic molecule. *Nature* **512**, 286–289 (2014).
18. Norrgard, E., McCarron, D., Steinecker, M., Tarbutt, M. & DeMille, D. Sub-millikelvin dipolar molecules in a radio-frequency magneto-optical trap. *Phys. Rev. Lett.* **116**, 063004 (2016).
19. Steinecker, M. H., McCarron, D. J., Zhu, Y. & DeMille, D. Improved radio-frequency magneto-optical trap of SrF molecules. *ChemPhysChem* **17**, 3664–3669 (2016).
20. Truppe, S. et al. Molecules cooled below the Doppler limit. *Nat. Phys.* **13**, 1173–1176 (2017).
21. Anderegg, L. et al. Radio frequency magneto-optical trapping of CaF with high density. *Phys. Rev. Lett.* **119**, 103201 (2017).
22. McCarron, D. J., Steinecker, M. H., Zhu, Y. & DeMille, D. Magnetically-trapped molecules efficiently loaded from a molecular MOT. Preprint at http://arXiv.org/abs/1712.01462 (2017).
23. Stellmer, S., Pasquiou, B., Grimm, R. & Schreck, F. Laser cooling to quantum degeneracy. *Phys. Rev. Lett.* **110**, 263003 (2013).
24. Hu, J. et al. Creation of a Bose-condensed gas of ^{87}Rb by laser cooling. *Science* **358**, 1078–1080 (2017).
25. Truppe, S. et al. An intense, cold, velocity-controlled molecular beam by frequency-chirped laser slowing. *New J. Phys.* **19**, 022001 (2017).
26. Devlin, J. A. & Tarbutt, M. R. Three-dimensional doppler, polarization-gradient, and magneto-optical forces for atoms and molecules with dark states. *New J. Phys.* **18**, 123017 (2016).
27. Grynberg, G. & Courtois, J.-Y. Proposal for a magneto-optical lattice for trapping atoms in nearly-dark states. *Europhys. Lett.* **27**, 41–46 (1994).
28. Sievers, F. et al. Simultaneous sub-Doppler laser cooling of fermionic ^{6}Li and ^{40}K on the D_1 line: theory and experiment. *Phys. Rev. A* **91**, 023426 (2015).
29. Burchianti, A. et al. Efficient all-optical production of large ^{6}Li quantum gases using D_1 gray-molasses cooling. *Phys. Rev. A* **90**, 043408 (2014).
30. Colzi, G. et al. Sub-Doppler cooling of sodium atoms in gray molasses. *Phys. Rev. A* **93**, 023421 (2016).
31. Kozyryev, I. et al. Sisyphus laser cooling of a polyatomic molecule. *Phys. Rev. Lett.* **118**, 173201 (2017).
32. Kosicki, M. B., Kedziera, D. & Zuchowski, P. S. Ab initio study of chemical reactions of cold SrF and CaF molecules with alkali-metal and alkaline-earth-metal atoms: the implications for sympathetic cooling. *J. Phys. Chem. A* **121**, 4152–4159 (2017).
33. Lim, J., Frye, M. D., Hutson, J. M. & Tarbutt, M. R. Modeling sympathetic cooling of molecules by ultracold atoms. *Phys. Rev. A* **92**, 053419 (2015).
34. Quéméner, G. & Bohn, J. L.. Shielding $^2\Sigma$ ultracold dipolar molecular collisions with electric fields. *Phys. Rev. A* **93**, 012704 (2016).
35. Schlosser, N., Reymond, G. & Grangier, P. Collisional blockade in microscopic optical dipole traps. *Phys. Rev. Lett.* **89**, 023005 (2002).
36. Yavuz, D. D. et al. Fast ground state manipulation of neutral atoms in microscopic optical traps. *Phys. Rev. Lett.* **96**, 063001 (2006).
37. Endres, M. et al. Atom-by-atom assembly of defect-free one-dimensional cold atom arrays. *Science* **354**, 1024–1027 (2016).
38. Barredo, D., de Léséleuc, S., Lienhard, V., Lahaye, T. & Browaeys, A. An atom-by-atom assembler of defect-free arbitrary two-dimensional atomic arrays. *Science* **354**, 1021–1023 (2016).
39. Vuletić, V., Chin, C., Kerman, A. J. & Chu, S. Degenerate Raman sideband cooling of trapped cesium atoms at very high atomic densities. *Phys. Rev. Lett.* **81**, 5768–5771 (1998).
40. Roos, C. F. et al. Experimental demonstration of ground state laser cooling with electromagnetically induced transparency. *Phys. Rev. Lett.* **85**, 5547–5550 (2000).
41. Kaufman, A. M., Lester, B. J. & Regal, C. A. Cooling a single atom in an optical tweezer to its quantum ground state. *Phys. Rev. X* **2**, 041014 (2012).
42. Thompson, J. D., Tiecke, T. G., Zibrov, A. S., Vuletić, V. & Lukin, M. D. Coherence and Raman sideband cooling of a single atom in an optical tweezer. *Phys. Rev. Lett.* **110**, 133001 (2013).

Author contributions

All authors contributed to all aspects of this work.

Competing interests

The authors declare no competing interests.

Additional information

Reprints and permissions information is available at www.nature.com/reprints.

Correspondence and requests for materials should be addressed to L.A.

Publisher's note: Springer Nature remains neutral with regard to jurisdictional claims in published maps and institutional affiliations.